JGR Biogeosciences

RESEARCH ARTICLE
10.1029/2023JG007832

Vegetation Loss Following Vertical Drowning of Mississippi River Deltaic Wetlands Leads to Faster Microbial Decomposition and Decreases in Soil Carbon

C. A. Creamer[1], M. P. Waldrop[1], C. L. Stagg[2], K. L. Manies[1], M. M. Baustian[3], C. Laurenzano[4,5], T. G. Aw[6], M. Haw[1], S. L. Merino[2], D. R. Schoolmaster Jr.[2], S. Sevilgen[1], R. K. Villani[3], and E. J. Ward[2]

[1]U.S. Geological Survey, Geology Minerals, Energy and Geophysics Science Center, Menlo Park, CA, USA, [2]U.S. Geological Survey, Wetland and Aquatic Research Center, Lafayette, LA, USA, [3]U.S. Geological Survey, Wetland and Aquatic Research Center, Baton Rouge, LA, USA, [4]Cherokee Nation System Solutions, Contractor to the U.S. Geological Survey, Wetland and Aquatic Research Center, Lafayette, LA, USA, [5]Now at Kathleen Babineaux Blanco Public Policy Center, University of Louisiana, Lafayette, LA, USA, [6]Department of Environmental Health Sciences, School of Public Health and Tropical Medicine, Tulane University, New Orleans, LA, USA

Abstract Wetland ecosystems hold nearly a third of the global soil carbon pool, but as wetlands rapidly disappear the fate of this stored soil carbon is unclear. The aim of this study was to quantify and then link potential rates of microbial decomposition after vertical drowning of vegetated tidal marshes in coastal Louisiana to known drivers of anaerobic decomposition altered by vegetation loss. Profiles of potential CH_4 and CO_2 production (surface to 60 cm deep) were measured during anaerobic incubations, organic matter chemistry was assessed with infrared spectroscopy, and soil porewater nutrients and redox potentials were measured in the field along a chronosequence of wetland loss. After vertical drowning, pond soils had lower redox potentials, higher pH values, lower soil carbon and nitrogen concentrations, lower lignin: polysaccharide ratios, more NH_4^+ and PO_4^{3-}, and higher rates of potential CO_2 release than vegetated marsh soils. Potential CH_4 production was similar in vegetated marshes and open water ponds, with depth-dependent decreases in CH_4 production as soil carbon concentrations increased. In these anoxic soils, vegetation loss exerts a primary control on decomposition rates because flooding drives sustained increases in porewater nutrient availability (NH_4^+ and PO_4^3, dissolved organic carbon) and decreases in redox potential (from −150 to −500 mV) that lead to higher potential CO_2 fluxes within a few years. Without new carbon inputs following wetland loss, the sustained decomposition in open water ponds may lead to losses of stored soil carbon and could influence global carbon budgets.

Plain Language Summary Coastal wetlands capture and store large amounts of carbon in soil and vegetation, but wetland ecosystems are being lost at a rapid rate. Coastal wetlands like tidal marshes can be lost when they flood and sink, which kills the marsh grasses in a process called vertical drowning. We found that microbial production of greenhouse gases was higher after marshes in coastal Louisiana vertically drown. These potential soil carbon losses were related to changing environmental conditions caused by the loss of marsh grasses, specifically increases in nutrient and organic matter availability and decreases in soil reduction-oxidation potential. A first impulse would be to think that at higher elevations, vegetated wetland soils would have faster rates of microbial decomposition than soils submerged under 10–70 cm of water. Our results show that the relationship between flooding and organic matter decomposition is more complex in tidal wetlands and suggest that faster decomposition rates combined with lower vegetation inputs following wetland loss could lead to sustained losses of previously stored soil carbon.

Key Points:

- The vertical drowning of coastal wetlands leads to stimulated rates of decomposition and higher production of CO_2
- Higher CO_2 production is mediated by vegetation loss, which is associated with lower redox potential and greater nutrient availability
- Without carbon inputs, sustained decomposition in open water ponds could lead to substantial losses of stored carbon

Supporting Information:

Supporting Information may be found in the online version of this article.

Correspondence to:

C. A. Creamer,
ccreamer@usgs.gov

Citation:

Creamer, C. A., Waldrop, M. P., Stagg, C. L., Manies, K. L., Baustian, M. M., Laurenzano, C., et al. (2024). Vegetation loss following vertical drowning of Mississippi River Deltaic wetlands leads to faster microbial decomposition and decreases in soil carbon. *Journal of Geophysical Research: Biogeosciences*, *129*, e2023JG007832. https://doi.org/10.1029/2023JG007832

Received 30 SEP 2023
Accepted 18 MAR 2024

Author Contributions:

Conceptualization: C. L. Stagg, D. R. Schoolmaster Jr., E. J. Ward
Data curation: C. L. Stagg, C. Laurenzano
Formal analysis: C. A. Creamer
Funding acquisition: C. L. Stagg
Investigation: C. A. Creamer, M. P. Waldrop, C. L. Stagg, K. L. Manies, M. M. Baustian, C. Laurenzano, T. G. Aw, M. Haw, S. L. Merino, S. Sevilgen, R. K. Villani, E. J. Ward
Methodology: C. A. Creamer, M. P. Waldrop, C. L. Stagg, K. L. Manies
Visualization: C. A. Creamer
Writing – original draft: C. A. Creamer, M. P. Waldrop, C. L. Stagg, K. L. Manies
Writing – review & editing: M. M. Baustian, C. Laurenzano, T. G. Aw,

1. Introduction

Wetland ecosystems are an important component of the global carbon cycle. Covering less than 10% of the Earth's land area, wetlands hold 20%–30% of the global soil carbon pool (Chmura et al., 2003; Choi & Wang, 2004). In addition to their large carbon stocks, coastal wetlands are an important carbon sink, accruing an estimated 5–87 Tg C per year globally (Chmura et al., 2003; Mcleod et al., 2011). However, in the past century an estimated 60%–70% of all wetland ecosystems have been lost due to combined pressures of sea level rise, land subsidence, and coastal development (Davidson, 2014; Duarte et al., 2008). In the conterminous United States, 80% of

wetland ecosystem losses have occurred in Louisiana (Bourne, 2000), due in part to the high rates of relative sea level rise in the region (DeLaune & White, 2012; Törnqvist et al., 2020). Roughly a quarter of the land area in coastal Louisiana has been lost in the last century (Couvillion et al., 2017) and the future of the remaining coastal wetlands is uncertain.

A primary mechanism of coastal wetland loss is vertical drowning (Blum et al., 2023; Saintilan et al., 2022). Vertical drowning occurs due to the disruption of hydrogeomorphic feedbacks between flooding, sediment accretion, and vegetation production that otherwise sustain the wetland's vertical position in the tidal frame (Kirwan & Megonigal, 2013; Morris et al., 2002; Schoolmaster et al., 2018). Excessive flooding causes declines in vegetation production or even complete mortality (Jones et al., 2021), reducing soil strength and wetland surface elevation (Cadigan et al., 2022), which reinforces the flooded condition and ultimately leads to conversion of vegetated marsh to open water (Chambers et al., 2019; Nyman et al., 1993; Stagg et al., 2020). The conversion of wetlands to open water can lead to direct and indirect losses of carbon, which vary by the mechanism of wetland loss. Lateral erosion can directly remove soil carbon through resuspension and export of the marsh soil (Sapkota & White, 2021). Following vegetation mortality from vertical drowning, soil carbon can decline due to a direct loss of carbon input (Schoolmaster et al., 2022a). The loss of vegetation also significantly alters biogeochemical cycling, which may lead to losses of stored carbon by changing microbial decomposition of existing soil carbon (DeLaune et al., 1994; Haywood et al., 2020). However, there is considerable uncertainty around the role microbial decomposition plays in controlling post-submergence soil carbon losses (Luk et al., 2023; Schoolmaster et al., 2022a).

Microbial decomposition is controlled by environmental, physicochemical, and biological factors that vary widely between wetland ecosystems (Schmidt et al., 2011; Spivak et al., 2019). Many of the abiotic and biotic controls on microbial decomposition can change—both abruptly and progressively—following ecosystem transitions (Stagg et al., 2017), and especially following disturbances (Luk et al., 2021). After wetland conversion into open water, soils become more anoxic, rates of sediment and nutrient delivery change, and microbial and plant communities die or change in composition (Neubauer & Megonigal, 2021). These altered abiotic and biotic conditions may have opposing effects on microbial decomposition (Stagg et al., 2018), resulting in ecosystem-specific responses to wetland loss (Kirwan et al., 2013; Spivak et al., 2019). Moreover, there is temporal decoupling in the complex feedbacks between hydrology, biogeochemistry, and geomorphology after wetland submergence, making predictions of ecosystem progression after wetland loss challenging (Fagherazzi et al., 2020; FitzGerald & Hughes, 2019; Neubauer et al., 2013). As a result, it is difficult to predict how much—and for how long—these conversions to open water will affect biogeochemical cycling rates and ultimately, carbon stocks in submerged soils.

In the Mississippi River Deltaic Plain, a model of wetland soil processes suggested that changes in carbon source inputs along with sustained microbial decomposition would lead to soil carbon losses after vegetated tidal marshes transition into open water (Schoolmaster et al., 2022a). We therefore proposed that the loss of vegetation that defines pond formation will have counter-balancing effects (direct and indirect) that ultimately result in no net change in decomposition rates. To test whether microbial decomposition changes over time following vertical drowning, we used a chronosequence (space-for-time substitution) of wetland loss to address the following hypotheses: (a) nutrient availability, particularly inorganic nitrogen, would increase with time following wetland loss due to limited plant N uptake in unvegetated ponds, stimulating microbial decomposition, and/or (b) a lack of new carbon inputs from plant litter deposition in open water ponds would be reflected in the organic matter chemistry of the recently accreted surface soils (≤25 cm), leading to progressively less decomposable carbon in open water ponds with time, slowing microbial decomposition.

2. Materials and Methods

2.1. Site Description

The field study was conducted on 15–17 October 2019 in a Louisiana salt marsh in the Barataria Hydrologic Basin, part of the Mississippi River Deltaic Plain, along the northern Gulf of Mexico coast (Figure 1). Surface water salinity varies widely in this area, and ranged from 4 to 22 ppt during the 2019 growing season and was 6.9 ppt at the time of sampling (CPRA of Louisiana, 2024). The average water level range in 2019 was 39.3 cm (90% = 42.1 cm, 10% = 2.7 cm), with a mean water level in 2019 of 21.3 cm (rectified to the North American Vertical Datum of 1988, NAVD88, in Geoid 12B) that ranged from 30.2 to 63.1 cm (NAVD88) at time of

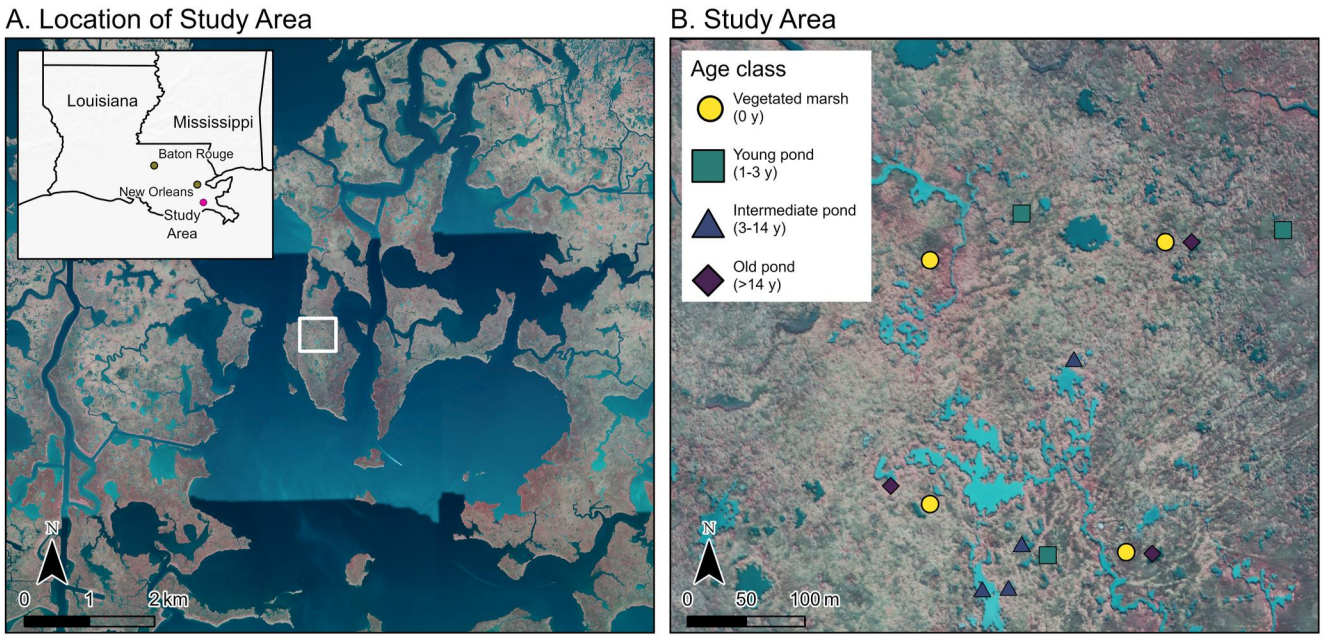

Figure 1. (a) Location of tidal marsh study area in coastal Louisiana (inset, pink dot) part of the Mississippi River Deltaic Plain (study area outlined by a white box), and (b) location of vegetated marshes and open water ponds (various ages). Basemap from NAIP (2024).

sampling (CPRA of Louisiana, 2024). The salt marsh sites contain a mosaic of vegetated marsh and open water ponds typical of natural coastal wetlands of Louisiana, USA. The vegetated marsh is dominated by salt tolerant grasses *Spartina alterniflora* Loisel and *Juncus roemerianus* Scheele, with *J. roemerianus* observed at higher elevations and the more flood tolerant *S. alterniflora* at lower elevations and adjacent to the open water ponds. Pond formation in this region is associated with prolonged flooding leading to vegetation mortality and conversion to open water (Cadigan et al., 2022). The time since pond formation was determined using land cover change analysis of high-resolution aerial imagery or digital orthophoto quarter quadrangles over a period of 21+ years (Schoolmaster et al., 2022a). A total of 14 sites were studied and we selected individual plots within four vegetated marsh sites and 10 open water pond sites (<20 m^2 in size), forming a chronosequence of wetland submergence. The vegetated marshes represent initial, pre-pond conditions (i.e., 0 years, $n = 4$). The open water pond sites were binned into the following age classes based on the time since pond formation: <3 years ($n = 3$), 3 ≤ 14 years ($n = 4$), and ≥14 years ($n = 3$). All sites were located within 300 m of one another (Figure 1) and co-located with a long-term Coastwide Reference Monitoring System station (CRMS0224, https://www.lacoast.gov/crms/Home.aspx), which provides over 15 years of sediment, vegetation, and hydrologic data, as well as Ameriflux site US-LA3 (29.4936, −89.9153, https://ameriflux.lbl.gov/sites/siteinfo/US-LA3) which provides annual carbon (CO_2, CH_4) and water fluxes.

Following the conversion of vegetated marsh to open water pond there was a significant decline in surface elevation associated with a loss of biomass structure and soil strength, characterizing marsh collapse (Cadigan et al., 2022). Therefore, vegetated marshes and open water ponds occupy different positions in the tidal frame. When expressed relative to the North American Datum of 1988 (NAVD88) the marsh soil surface is 20–22 cm above NAVD88, while the open water ponds are 5–15 cm below NAVD88. As such, the open water ponds experience longer and deeper flooding while vegetated marshes experience larger daily and annual water level fluctuations (Chambers et al., 2019; Stagg et al., 2020). To reflect the dominant control of position within the tidal frame (rather than distance from the sediment surface), all sampling depths (porewater and sediment cores) were expressed relative to NAVD88 elevation-adjusted depth, where positive values are above NAVD88 and negative values below the datum. Sediment surface elevation was rectified to NAVD88 using high-resolution real-time kinematic elevation surveys at each sampling location (Cadigan et al., 2022). Because for some data types, notably reduction-oxidation potential and methane production, depth from the sediment surface is important, some data are also presented relative to absolute depth (i.e., distance from the sediment surface) in the Supporting Information S1.

2.2. Porewater Collection

Field data was collected at all 14 sites. Samples were collected from a raised platform in vegetated marsh sites, and from the side of an airboat in the open water pond sites. Surface water temperature, measured with a digital pocket thermometer, was 26 ± 2.8°C across all sites. The depth of ponded water above the sediment surface ranged from 10–70 cm across all 10 sites (Stagg et al., 2024). Reduction-oxidation potential (redox) was measured using platinum electrode redox probes (Faulkner et al., 1989). Three replicate redox probes were installed to each of three depths (10, 30, and 50 cm) below the surface of the sediment at each site (i.e., 3 redox measurements collected for each pond and vegetated marsh). Redox probes were equilibrated for at least 30 min before recording. We sampled porewater at these same depths, with an additional sample at 70 cm below the sediment surface in vegetated marshes. We also collected four surface water samples to measure nutrients in the source water. All porewaters were sampled using a fritted stainless-steel rod (1-cm outer diameter), three-way stopcock, and a 60-mL plastic syringe. A 30-mL rinse sample was collected and discarded, and then a 60-mL porewater sample was collected into the syringe, then syringe filtered to <0.2 μm using a glass fiber triple filter (ADPV25RB, Omicron scientific, Alpharetta, GA). Approximately 30 mL of the sample was injected into a pre-evacuated 30-mL serum vial crimp-sealed with butyl rubber septa. Vials were refrigerated and shipped to Menlo Park, CA for analysis. Dissolved organic carbon (DOC) from the porewater sample was measured within 4 days of field collection and the remaining dissolved constituents were measured within 2 weeks. DOC was measured by high temperature combustion using a total organic carbon analyzer (TOC-VCPH analyzer, Shimadzu, Japan). Nitrate and nitrite (NO_3^-/NO_2^-), ammonium (NH_4^+), and phosphate (PO_4^{3-}) were quantified by automated spectrophotometry (Aquakem250, Thermo Fisher Scientific, United States). Nitrate-nitrite was quantified using the enzymatic reduction method (Patton & Kryskalla, 2011), NH_4^+ by EPA method 350.1 (U.S. EPA, 1993a) and PO_4^{3-} by EPA Method 361.5 (U.S. EPA, 1993b). Sulfate was measured by high performance ion chromatography (Metrohm 881 Compact IC pro, Metrohm AG, Switzerland) with a Metrosep A Supp 7/250 column following EPA test method 9056A (U.S. EPA, 2007).

2.3. Sediment Collection

After collection of porewater, sediments were collected from each of the 14 sites with a McCauley corer (i.e., Russian peat corer; half-cylinder, 5.1-cm diameter, 100-cm length). Prior to each sampling, the corer was rinsed with marsh water and then bleach sterilized. In both marsh and open water sites, the top of the core corresponds to the top of the sediment: the corer was submerged in all open water ponds. The corers were placed on the bow of the airboat, opened, and the sediments were visually characterized and subsampled. Sediments were segmented using bleach sterilized knives and scissors into the following depth increments relative to the sediment surface: 0–20 cm, 20–40 cm, and 40–60 cm at all sites and with an additional 60–80 cm segment in vegetated marshes. Each of the 20-cm sediment sections were laterally split in the field. One half was collected into sterile 50-mL Falcon tubes and immediately frozen on dry ice for sample characterization (described below). These samples remained frozen throughout field sampling, were shipped on dry ice to Menlo Park, CA for analysis, and remained frozen at −20°C until processed. The other half of each section was homogenized in the field using a manual food processor (Cuisinart Prep Express, 3 grinding pulls per sample). We weighed approximately 30 g of the homogenized water-saturated sediment into pre-tared 240 mL borosilicate glass serum vials and then crimp-sealed the vials with butyl rubber septa. The vials were immediately purged with ultra-high purity N_2 gas for 5 min at an approximate flow rate of 500 mL min^{-1} to decrease headspace O_2. We weighed the vials after sediment addition (before crimp-sealing) and after flushing (with crimp seals). The vials were stored in a cooler with ice packs in the field and stored at 4°C for one to 3 days prior to shipping overnight in coolers with ice packs to Menlo Park, CA for analysis.

2.4. Sediment Characterization

We quantified nutrient concentrations (carbon, nitrogen), pH values, and organic matter composition (using infrared spectroscopy) of each sediment depth increment. Samples were freeze-dried and the sediment water content was determined by mass loss. Soil pH was measured after shaking with deionized water (1:5 w/v). Dried samples were ground to pass an 80-mesh sieve (<177 μm) and analyzed for total carbon and nitrogen by high temperature combustion (Carlo Erba NA1500 elemental analyzer, Thermo Scientific, Waltham, MA). A lack of effervescence after adding 4 M HCl indicated all carbon was organic (Nelson & Sommers, 1996). Bulk density

across the depth increments was estimated by averaging values measured in a replicate core from the sites (Schoolmaster et al., 2022b).

Organic matter chemistry of sediment samples was qualitatively assessed using attenuated total reflection with infrared spectroscopy (ATR-IR). Spectra were collected from pellet pressed samples using a Nicolet iN10 Microscope and iS20 Fourier Transform (FT)-IR spectrometer with a liquid nitrogen cooled Mercury-Cadmium-Telluride (MCT) detector and a germanium crystal (Thermo Fisher Scientific). Mid-infrared (mid-IR) absorbance spectra were collected for each pressed sample by averaging the spectra from three randomly selected points within a 400 × 400 μm square. At each point, we collected 16 five-second scans from 675 to 4,000 cm^{-1} with 4 cm^{-1} spectral resolution. Background spectra were collected before each sample under the same conditions. We applied an atmospheric correction and ATR correction for a germanium crystal in the associated OMNIC Picta Software (v1.0). ATR corrected spectra were detrended (third order polynomial), baseline corrected (offset and linear), and normalized in Unscrambler X (10.4.1). Corrected spectra are provided in Stagg et al. (2024). We calculated lignin: polysaccharide ratios using the height of peaks centered at 1,515 cm^{-1} (aromatic C = C stretch; lignin) and 1,035 cm^{-1} (C-O-C and C-OH stretching; polysaccharides) (Calderón et al., 2013; Parikh et al., 2014). In organic sediments (>10% organic carbon), lower lignin: polysaccharide ratios can indicate a greater potential for decomposition (Hodgkins et al., 2014; Waldrop et al., 2021).

2.5. Anaerobic Incubations

The serum vials containing the saturated marsh sediments were incubated under anoxic conditions and in the dark at 23°C (±0.38°C) for 3 months (91 days). Within 24 hr of arrival in the lab, the incubation vials were evacuated (5 times, −75 kPa) and filled to atmospheric pressure (100 kPa) with ultra-high purity N_2 to initiate the incubation. Each week, the incubation vials were evacuated and re-filled with ultra-high purity N_2. Vial headspace was typically sampled 2 and 7 days later. We calculated weekly GHG (greenhouse gas: CO_2, CH_4, N_2O) production rates as the difference in concentrations between the two sampling points (day 2 and day 7). During the first 2 weeks of the incubation, samples were collected more frequently (i.e., days 2, 5, and 7). Headspace samples were collected from the incubation vials in a glove bag atmosphere (N_2 atmosphere with and $H_2 \geq 1.5\%$, oxygen monitored and at 0 ppm) and injected into N_2 flushed 20 mL crimp-sealed sample vials for analysis.

We quantified CO_2 (≥500 ppm), CH_4 (≥5 ppm), and N_2O (≥2.5 ppm) in the sample vials by gas chromatography (8610C, SRI Instruments, Torrance CA). Nitrous oxide (N_2O) was below detection during the entire incubation (calibration curve from 0–10 ppm), these data are not presented. The incubation vials were weighed at the start of the incubation (upon arrival in the lab), after each flushing, and at the end of the incubation to quantify any change in water content. Water content (g water · g $sediment^{-1}$) varied by no more than ±3% during the incubation (the average water content was 0.6% lower than starting values by the end of the incubation). At the end of the incubation, the crimp tops and rubber septa were removed in an aerobic atmosphere and the soils were oven-dried for 21 days at 60°C (until all samples reached constant weight).

2.6. Calculations

We determined microbial GHG (CO_2 and CH_4) production from the wetland sediments during the incubation by quantifying GHG in the headspace over time and correcting for the pressure within each vial and the partitioning of CO_2 and CH_4 between liquid and aqueous phases. All incubation vials were over-pressurized for the first headspace sample (2 days after flushing-N_2 filling: average pressure of 1.15 ± 0.07 atm). Because we did not replace sampled headspace after the first gas sample, the pressure in the incubation vials was always lower for the second gas sample (average of 1.00 ± 0.06 atm). For vials that were not over-pressurized at the second gas sampling we calculated the incubation vial pressure by subtracting the headspace volume removed by the first headspace sample. We used these over- or under-pressurization volumes to calculate the pressure in the vials using Boyle's law. Gas concentrations (mol L^{-1}) were then calculated using known pressures and temperatures of the vials. To calculate GHG in the aqueous phase, we used Henry's Law solubility constants for CO_2 (0.034 mol L-atm^{-1} at 298.15 K) and CH_4 (0.0021 mol L-atm^{-1} at 298.15 K) modified for the ambient temperature of our incubators (23°C) using the van 't Hoff equation and temperature dependence constants for CO_2 (2400 K) and CH_4 (1750 K) (Harvey & Smith, 2007; Sander, 2015). The amount of GHG in the aqueous phase (moles) was added to the amount of GHG in the gaseous phase (moles) to calculate the total quantity of GHG emitted each week and the cumulative amount of GHG produced during the full incubation period.

Soil biogeochemical models (e.g., CENTURY, RothC) divide soil carbon into discrete pools that decompose at different rates (e.g., Coleman & Jenkinson, 1996; Parton et al., 1994). The size and turnover rate of these conceptual but measurable carbon pools can be approximated from respiration dynamics measured during laboratory incubations (Paul et al., 2001). We used a two-pool exponential decay model that fits an actively cycling pool (decay rates of days to weeks) and a slower-cycling pool (decay rates of years to decades) with our incubation data (Schädel et al., 2013) using the equation:

$$c_{\text{total}} = c_a \times \left(1 - \exp^{(-k_a t)}\right) + c_s \times \left(1 - \exp^{(-k_s t)}\right) \quad (1)$$

where t is time (in days), k is the decay rate (in days^{-1}) and C is pool size of the active (a) and slow (s) carbon pools, and *total* is the cumulative amount of CO_2 respired. The mean residence time of the carbon pools was calculated as the inverse of the decay rate. Because derived parameters from incubations are sensitive to the length of the incubation (Hamdi et al., 2013), estimates of slow pool dynamics are more uncertain from our short-term incubation (c.a. 90 days). Patterns in CH_4 release did not follow a bi-phasic pattern but instead were generally consistent throughout the incubation. However, some surface samples had declines in CH_4 production with time, while some samples at depth began producing small quantities of CH_4 at later stages in the incubation (e.g., after 30 days), likely due to depletion of terminal electron acceptors during the incubation. Because CH_4 release at depth was minor relative to surface sediments, cumulative CH_4 production includes all timepoints.

2.7. Statistics

We used a linear mixed effects model to examine changes in soil carbon, soil nitrogen, bulk density, soil pH, lignin: polysaccharide ratios calculated from mid-IR data, GHG emissions, and porewater constituents as a function of wetland type (i.e., vegetated marsh vs. open water pond) and elevation-rectified sampling depth, with individual plots (i.e., a specific pond or vegetation marsh location) specified as a random effects using the lme4 package (version 1.1–34; Bates et al., 2015). Data were transformed with a Box-Cox (lignin: polysaccharide ratios) or log transformation (CH_4 release) so model residuals were normally distributed. We used the same approach to determine whether the time since marsh loss (also referred to as pond age, with vegetated wetlands having a pond age of 0 years) better described changes in the data than wetland type (i.e., we replaced pond age with wetland type in the linear mixed effects model). Only the porewater nutrients DOC, NH_4^+, PO_4^{3-} changed as a function of time since marsh loss independent of sampling depth (i.e., not just the transition from vegetated marsh to open water pond). For these data with non-linear relationships to pond age, we fit a generalized additive model (GAM) of the data relative to the years since marsh loss, with generalized cross validation (GCV) for smoothing (thin plate splines) using the mgcv package (version 1.8–41; Wood, 2017). The non-linear relationship between cumulative CO_2 release and sampling depth in vegetated marshes was also fit with a GAM model, as it provided a significantly better fit than a linear regression (evaluated using ANOVA). These statistics were conducted in R and R Studio (version 2023.03.01; R Core Team, 2014). All values in text are means ± standard deviations unless otherwise indicated. We used principal components analysis to identify regions of the full IR spectra (675–4,000 cm^{-1}) that distinguished our samples in Unscrambler X (10.4.1).

We used partial least squares (PLS) regression to identify whether a combination of the measured environmental variables (e.g., organic matter concentrations, porewater constituents), represented as components (or latent variables), could predict CH_4 and CO_2 production during the incubation. We used the model developed by Schoolmaster et al. (2022b) as the basis for predictor variable selection in the PLS approach. We conducted PLS analysis in Unscrambler X (10.4.1) with the NIPALS algorithm. We used the smallest number of components for the PLS regression that achieved a local minimum in the root mean square error (RMSE). The RMSE and variance explained are shown for the calibration and validation data in text. We used cross-validation of 20 random segments, and jack-knife estimation of the uncertainty in the regression model coefficients (beta coefficients) for each predictor variable. Predictor variables with large positive or negative regression model coefficients are more important in the regression model. The uncertainty in estimated regression model coefficients was used to determine whether a predicting environmental variable was a significant component in the model.

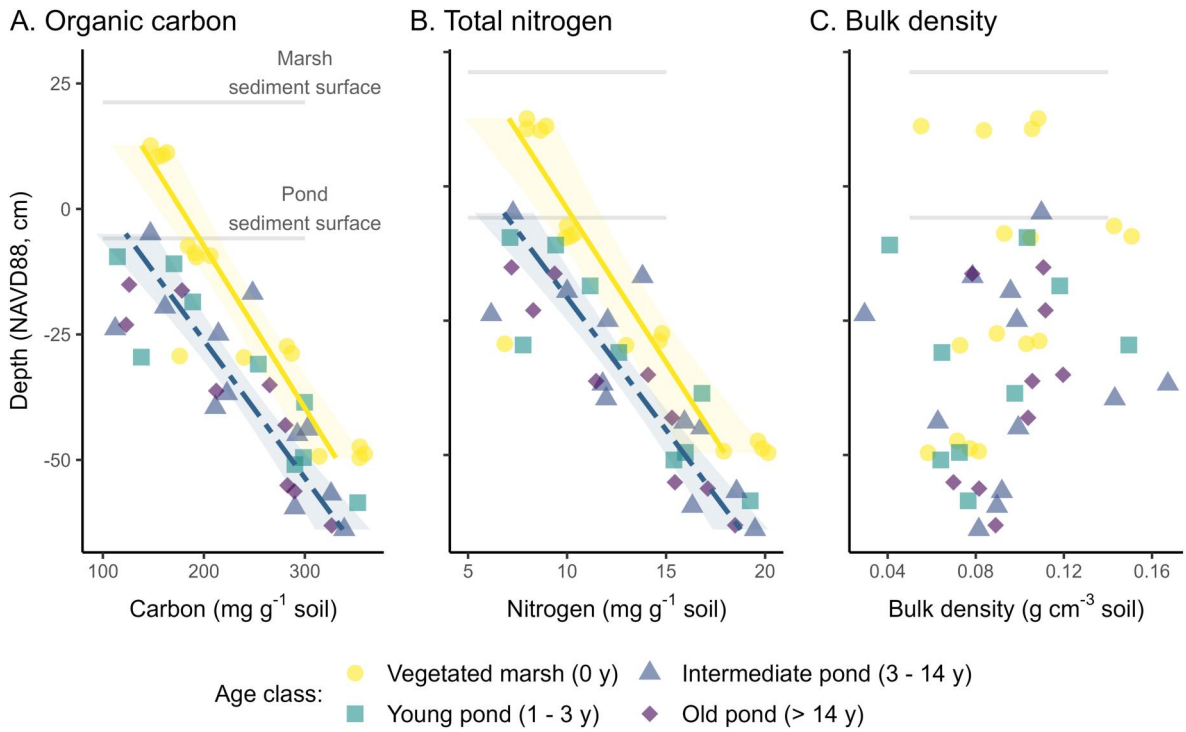

Figure 2. Soil (a) organic carbon and (b) total nitrogen concentrations and (c) and bulk densities through depth in vegetated marshes and open water ponds. Linear regressions for vegetated marshes and open water ponds are shown with 95% confidence intervals for carbon ($R^2 = 0.83$ and 0.74, respectively) and nitrogen ($R^2 = 0.74$ and 0.77, respectively) relative to depth. Bulk density was unrelated to depth. Sample depth is shown relative to NAVD88 elevation of the soil surface. The average NAVD88 elevation of the soil surface in vegetated marshes ($n = 4$) and open water ponds ($n = 10$) are shown as gray lines. All figure data can be found in Stagg et al. (2024).

3. Results

3.1. Carbon, Nitrogen, and Lignin: Polysaccharide Ratios Increase With Depth

Carbon and nitrogen concentrations increased down the soil profile in both vegetated marshes and open water ponds ($P < 0.001$; Figures 2a and 2b). Although the pattern of increasing organic matter concentrations with depth were similar across marshes and ponds, soil carbon and nitrogen concentrations were lower in the open water ponds than in vegetated marshes (carbon $P = 0.006$; nitrogen $P = 0.004$). The decrease in carbon and nitrogen concentrations at equivalent elevation-adjusted depths occurred within 1–3 years of wetland loss, without additional decreases as pond age increased. Bulk density was relatively consistent throughout the soil profile and in vegetated marshes and open water ponds, ranging from 0.03–0.17 g cm^{-3} (Figure 2c). Changes in carbon and nitrogen densities (i.e., g cm^{-3}) therefore showed similar ecosystem and depth-dependent patterns as carbon and nitrogen concentrations, although whole-profile carbon stocks to 1 m below the sediment surface (i.e., not densities or concentrations) are similar between vegetated marshes and open water ponds (Schoolmaster et al., 2022b).

The ratio of mid-IR spectra peaks associated with lignin (1,515 cm^{-1}) relative to polysaccharides (1,035 cm^{-1}) were marginally lower in open water ponds than in vegetated marshes ($P = 0.11$) and progressively increased with depth ($P < 0.001$; Figure 3). A PCA of the entire mid-IR spectra of the sample explained 94.6% of the variance in the data, with 92.5% of the variance explained by PC1 (Figure 3b). A peak centered at 1,035 cm^{-1} indicative of C-O-C and C-OH stretching (a polysaccharide proxy; Calderón et al., 2013; Parikh et al., 2014) had the strongest positive loadings for PC1 (i.e., contributed the most to the separation of mid-IR spectra along PC1; Supporting Information S1). Depth (Pearson's $r = 0.67$) and organic matter concentrations (carbon or nitrogen; Pearson's $r = -0.85$) were highly correlated with PC1. These results reveal that surface soils were potentially more decomposable compared to the deeper soils with higher carbon concentrations but lower polysaccharide content.

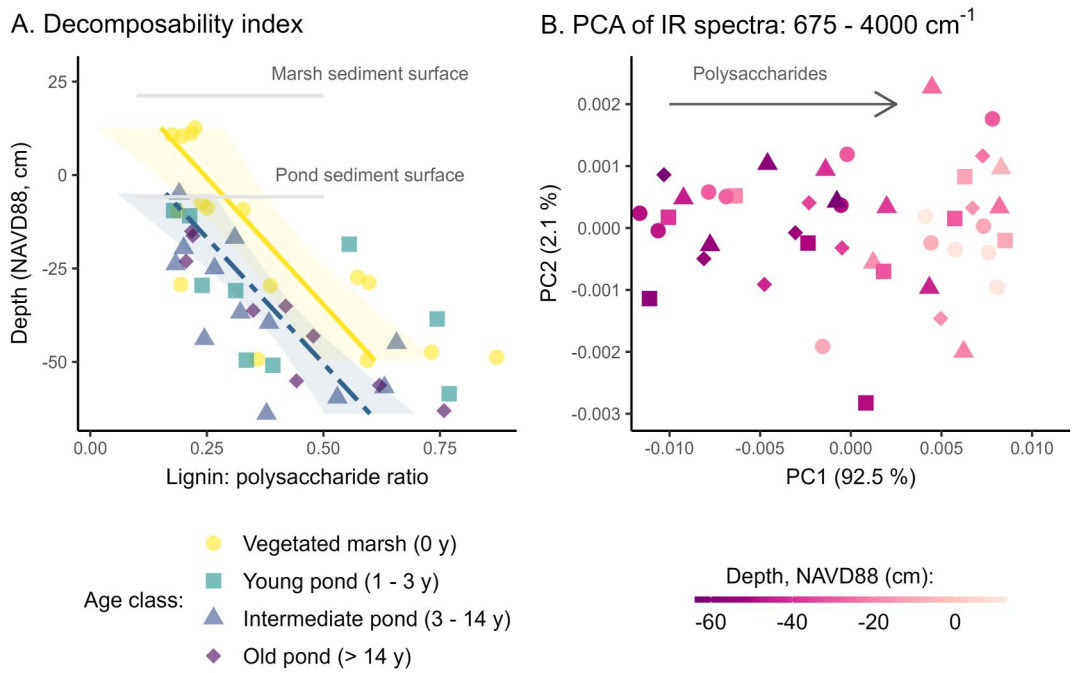

Figure 3. Depth-dependent changes in organic matter chemistry proxied with mid-infrared spectroscopy. The (a) decomposability index, or the ratio of infrared regions associated with C = C (lignin proxy) and C-O-C/C-OH (polysaccharide proxy), increased with depth in vegetated and open water ponds. Assumed decomposability is higher at lower lignin: polysaccharide ratios. Linear regressions of lignin: polysaccharide ratios relative to depth are shown for vegetated marshes ($R^2 = 0.56$) and open water ponds ($R^2 = 0.47$) with 95% confidence intervals. The (b) depth-dependent separation of the samples using PCA of entire spectra (675–4,000 cm^{-1}) results from positive loadings in the polysaccharide region (1,030–1,080 cm^{-1}) along PC1.

3.2. Porewater NH_4^+ and PO_3^- Increase While Redox Potential Decreases After Vertical Drowning and Wetland Loss

The pH value of the soils was neutral, ranging from 6.65 ± 0.43 in vegetated marshes to a slightly higher value of 6.85 ± 0.37 in the open water ponds ($P = 0.038$, Supporting Information S1). The redox in these soils was low, less than −150 mV, indicating the soil is anoxic at all measured depths in both vegetated marshes and open water ponds (Figure 4a). Sediments in the ponds were more reducing (i.e., lower redox potential) than the marsh soils ($P = 0.029$), and redox potential decreased significantly with depth ($P < 0.001$). There were no measurable changes in redox potential with soil depth in the vegetated marshes ($P = 0.61$). Despite being dominated by typical salt marsh vegetation, at the time of sampling the surface waters had only 8.7 ± 0.2 mg L^{-1} of SO_4^{3-}, compared to 100–500 mg L^{-1} range measured in other saline marshes (Bartlett et al., 1987; Poffenbarger et al., 2011). Soil porewater SO_4^{3-} concentrations were also low, averaging 1.8 ± 1.6 mg L^{-1} across all depths and pond ages (including vegetated wetlands with a pond age of 0 years; Supporting Information S1). Porewater and surface water NO_3^- and NO_2^- were also low across all depths and pond ages, with concentrations less than 0.35 mg L^{-1} (Supporting Information S1). As a result, NH_4^+ was the dominant form of inorganic N in the soil porewater, and NH_4^+ increased with the time since marsh loss (Figure 4b). Porewater phosphate showed similar, but more variable, increases following the conversion of vegetated marshes to open water ponds (Figure 4c). Porewater DOC was moderately correlated with NH_4^+ and PO_4^{3-} (Pearson's $r \geq 0.71$) but was more variable, ranging from 6–41 mg C L^{-1}, and therefore showed only marginal increases following vertical drowning ($P = 0.06$; Supporting Information S1). Surface water concentrations of NH_4^+ (0.03 ± 0.02 mg L^{-1}), PO_4^{3-} (0.14 ± 0.24 mg L^{-1}), and DOC (below detection) were lower than porewater concentrations.

3.3. CH_4 Production Decreases With Depth

The cumulative amount of CH_4 produced during the incubation period was insensitive to wetland loss, with indistinguishable rates between vegetated marshes and open water ponds (Figure 5a). Instead, CH_4 production

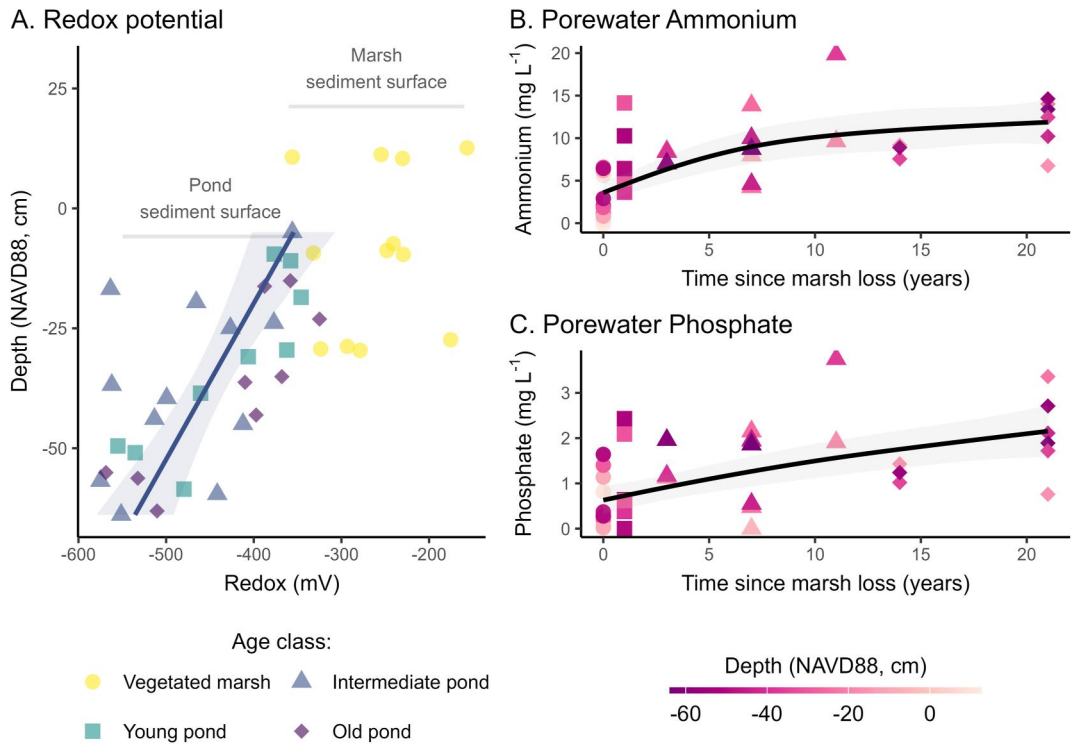

Figure 4. (a) Redox potential and (b) porewater concentrations of NH_4^+ and (c) PO_4^{3-} during the conversion of vegetated marshes to open water ponds. Linear regressions of redox potential with depth are shown for open water ponds ($P < 0.001$; $R^2 = 0.61$) with 95% confidence intervals. Vegetated marshes have no significant relationship with depth. Generalized additive models (GAM) of increasing NH_4^+ ($P < 0.001$, $R^2 = 0.45$) and PO_4^{3-} concentrations ($P < 0.001$; $R^2 = 0.51$) relative to time since marsh loss are shown with 95% confidence intervals. The average NAVD88 elevation of the soil surface in vegetated marshes ($n = 4$) and open water ponds ($n = 10$) are shown as gray lines in (a). Unlike soil and porewater samples, redox potential could not be collected 70 cm below the sediment surface in vegetated marshes. See Supporting Information S1 for redox potential relative to depth below the sediment surface.

was dependent on depth ($P < 0.001$), with the upper sections of each soil profile, corresponding to the top 40 cm of sediment in the vegetated marshes and the top 20 cm of sediment in the ponds (i.e., at depths shallower than 25 cm below NAVD88), releasing 20 to 100 times more CH_4 than soils deeper in the profile (Supporting Information S1). We used PLS regression to determine which measured variables were related to log-transformed quantities of cumulative CH_4 produced per g soil during the incubation. The regression model explained 59% of the variation in the log of CH_4 production from vegetated marshes and open water ponds (calibration: RMSE = 0.83; validation: RMSE = 0.91 and 54% explained variance). Organic carbon was the most important variable in the regression and alone could explain 57% of the variation in CH_4 production (Figure 5c). Three additional components, gravimetric soil water content ($P < 0.001$), lignin: polysaccharide ratio ($P < 0.001$) and soil N concentration ($P = 0.001$) also contributed to the PLS regression, but their regression coefficients were comparatively small (Figure 5b). Taken together, soils more than 25 cm below NAVD88— which roughly have more than 20% organic carbon, less than 1% nitrogen, and lignin: polysaccharide ratios greater than 0.3—produced little to no CH_4 during the anaerobic incubation.

3.4. CO_2 Production Increases After Vertical Drowning and Wetland Loss

The cumulative amount of CO_2 produced per g of soil during the incubation was higher in open water ponds than in vegetated marshes ($P = 0.01$; Figure 6a). Unlike CH_4, CO_2 production per g of soil only changed with depth in the vegetated marshes. However, because soil carbon concentrations increase with depth (Figure 2a), proportionately less soil C was respired as CO_2 at depth in both vegetated marshes in open water ponds. In surface soils, between 1% (ponds) and 0.75% (vegetated marshes) of soil C was respired as CO_2 during the 3-month incubation. Loss of soil C as CO_2 declined to about 0.25% at depth in both ponds and vegetated marshes (Supporting Information S1). We estimated CO_2 release dynamics during the incubation on a per g soil basis using a two-pool

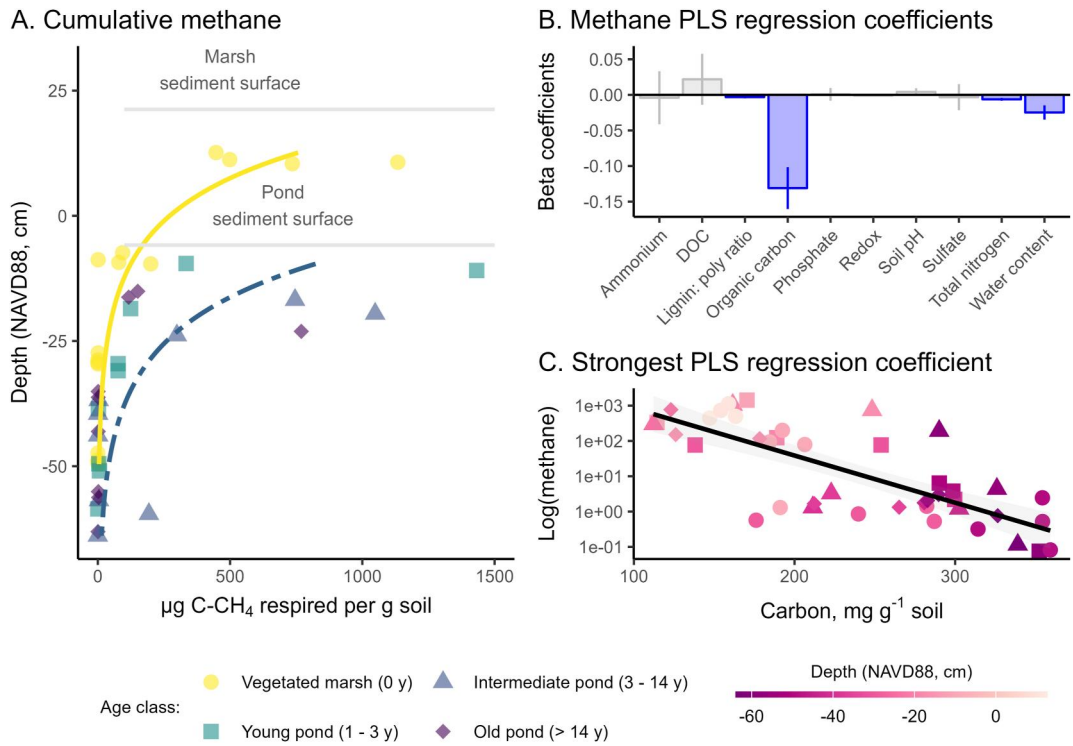

Figure 5. Patterns and drivers of cumulative CH_4 release during the incubation in vegetated marshes and open water ponds. (a) First order exponential fits of decreases in CH_4 production with depth are shown for vegetated marshes ($P \leq 0.01$, pseudo-$R^2 = 0.76$) and open water ponds ($P \leq 0.01$, pseudo-$R^2 = 0.45$). The average NAVD88 elevation of the soil surface in vegetated marshes ($n = 4$) and open water ponds ($n = 10$) are shown as gray lines. (b) Significant environmental variable coefficients related to CH_4 production from the PLS regression model are shown in blue (59% of variation with 3 factors). (c) Soil carbon is the most important predictor of cumulative methane release during the incubation ($P < 0.001$, $R^2 = 0.57$).

exponential model (Equation 1) that classifies decomposing organics into faster and slower cycling pools (Paul et al., 2001) (Supporting Information S1). Reflecting patterns in cumulative CO_2 release, the size of the faster cycling carbon pool marginally increased after vertical drowning ($P = 0.02$; 140 ± 70 μg C- CO_2 per g of soil in vegetated marshes vs. 360 ± 240 μg C- CO_2 per g of soil in open water ponds; Supporting Information S1). This faster cycling pool—which represents more easily decomposable sources of microbial and plant carbon—had a mean residence time of 4–9 days across all depths and pond ages (including vegetated marshes with a pond age of 0 years). Although the size of the slow cycling pool was consistent across pond ages and depths (average of 1,120 ± 510 μg of C per g soil), its decay rate increased with depth. In vegetated marshes, the residence time of the slow pool declined linearly ($P < 0.001$, $R^2 = 0.85$) from about 100 days at the surface to 40 days at depth, while the residence time of the slow pool in ponds only declined from about 75 days at the surface to 60 days at depth (Supporting Information S1). Taken together, these estimated pool sizes and decay rates suggest that after vertical drowning, a larger and faster cycling of carbon pool allows for greater CO_2 fluxes from pond soils relative to vegetated marsh soils.

We used PLS regression to determine which measured variables (porewater chemistry, organic matter concentrations, redox potential) were related to patterns of cumulative CO_2 release in the vegetated marshes and open water ponds. The PLS regression model explained 29% of the variation in CO_2 released per g of soil with one factor (calibration: RMSE = 297; validation: RMSE = 312 with 25% explained variance). Redox ($P < 0.001$), NH_4^+ ($P = 0.009$), gravimetric water content ($P = 0.001$), PO_4^{3-} ($P = 0.014$), and DOC ($P = 0.015$) were significant variables in the regression model (Figure 6b). Although increases in NH_4^+, PO_4^{3-}, and DOC increased CO_2 production (i.e., positive regression coefficients), redox was the most important predictor of CO_2 production, where more CO_2 was released at lower (i.e., more negative) redox potentials (Figure 6c). However, the majority of variance in CO_2 production (71%) could not be explained by any of our measured environmental variables.

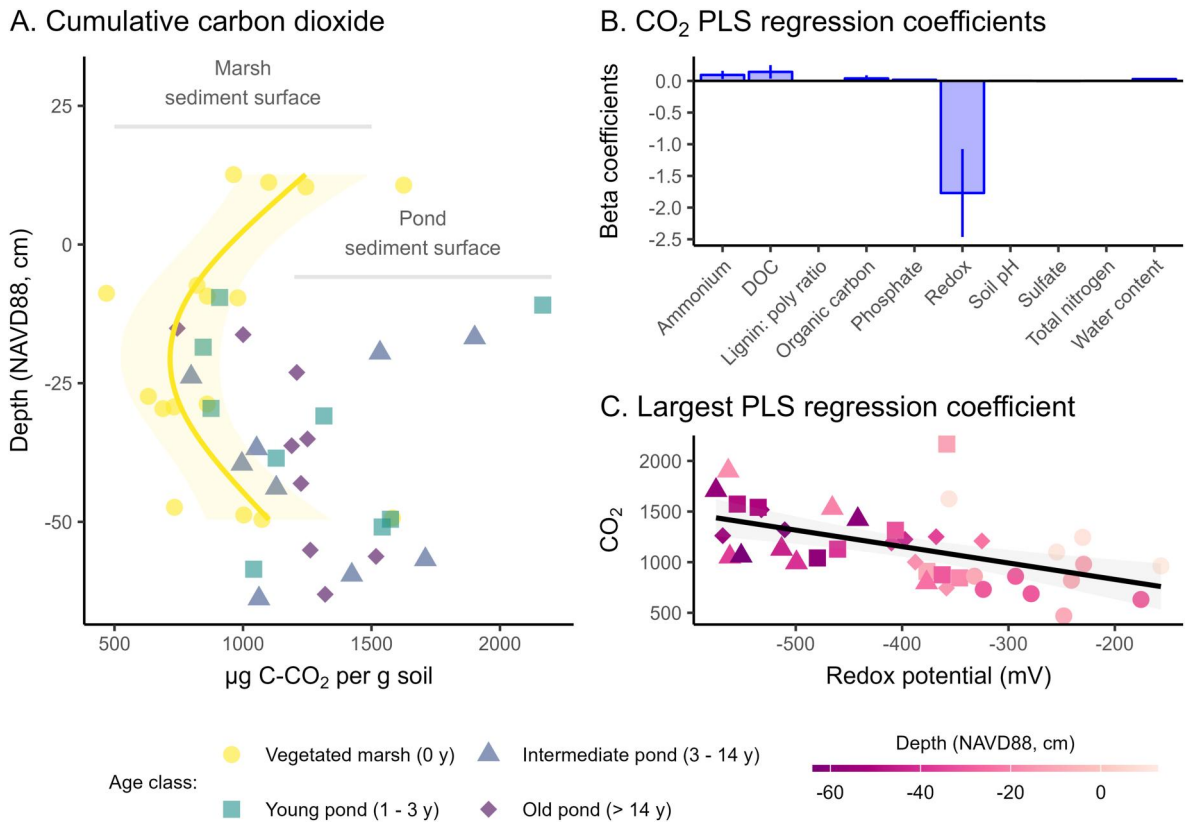

Figure 6. Patterns and drivers of cumulative CO_2 release during the incubation in vegetated marshes and open water ponds. (a) Generalized additive model (GAM) of CO_2 production relative to depth is shown for vegetated marshes with 95% confidence intervals ($P = 0.02$, $R^2 = 0.39$). CO_2 production is not significant relative to depth in ponds. The average NAVD88 elevation of the soil surface in vegetated marshes ($n = 4$) and open water ponds ($n = 10$) are shown as gray lines. (b) Significant environmental variable coefficients related to CO_2 production from the PLS regression model are shown in blue (29% of variation with 1 factor). (c) Redox potential was the most important predictor of cumulative CO_2 release during the incubation ($P < 0.001$, $R^2 = 0.26$).

4. Discussion

4.1. Biogeochemical Changes During Transition From Vegetated Marsh to Open Water Ponds

Nutrient availability in wetland soils is tightly coupled to flood regime, redox status, and plant-soil interactions (Neubauer & Megonigal, 2021; Patrick & DeLaune, 1977; Reddy et al., 2000). The conversion of vegetated marsh to open water pond is characterized by not only the loss of vegetation, but also longer and deeper flooding (Chambers et al., 2019; Stagg et al., 2020), both of which can impact redox status and nutrient cycling. At the time of sampling, both the vegetated marshes and open water ponds were highly reducing at 10 cm soil depths (i.e., the shallowest depth measured with our redox probe), and redox potentials decreased further with sediment depths in the ponds (Figure 4a). Vegetated marshes, dominated by *Spartina alterniflora* (smooth cordgrass) and *Juncus roemerianus* (needlegrass rush), had higher soil redox potentials than the ponds, and the redox potential was insensitive to sampling depth. The similar (and low) redox potentials through depth in the vegetated marshes were likely because the wetlands were flooded at the time of sampling (CPRA of Louisiana, 2024). Tidal marsh redox potentials can change substantially (>300 mV) over 1–2 days in response to inundation (Catallo, 1999), and so the measured redox potentials reflected the flooded conditions at the time of sampling. However, the measured differences in marsh and pond redox potential persisted despite the higher-than-average water levels. Due to the vegetated marshes being about 20 cm higher in elevation than the ponds (Cadigan et al., 2022), there is more drainage during low tide and higher redox potentials (Stagg & Mendelssohn, 2010). Additionally, living roots and rhizomes of *Spartina* and *Juncus*, which can reach to 30–60 cm soil depths and form aerenchyma (Materne et al., 2022), can oxidize soils and increase redox potentials (Howes et al., 1981; Jaynes & Carpenter, 1986; Koretsky et al., 2008; Wolf et al., 2007). As a result, the removal of vegetation following vertical drowning can lead to significant declines in redox potential (de la Cruz et al., 1989; Mueller et al., 2016).

In both vegetated and ponded areas, the concentrations of the porewater nutrients NO_3^-, NO_2^-, NH_4^+, SO_4^{2-}, and PO_4^{3-} reflected known patterns for highly reducing environments of submerged soils: SO_4^{3-}, NO_3^-, and NO_2^- concentrations were low while PO_4^{3-} and NH_4^+ were high (Figure 4, Supporting Information S1) (Marschner, 2021; Patrick & DeLaune, 1977). Following wetland loss, porewater NH_4^+ and PO_4^{3-} concentrations increased with time. Given that nutrient delivery is similar among the hydrologically connected vegetated marshes and ponds (Figure 1), the production and/or uptake of ammonium and phosphate was altered following the conversion of vegetated marsh to open water pond. Phosphate solubility increases at low redox potentials (≤100–200 mV) due to reduction of insoluble Fe(III) to soluble Fe(II), which releases co-precipitated PO_4^{3-} (Guo et al., 2000; Patrick & DeLaune, 1977). This increase in Fe solubility is likely responsible in part for higher porewater PO_4^{3-} in the more reduced open water ponds. Ammonium typically accumulates in wetland porewaters (Reddy et al., 2000) as microbes release NH_4^+ during anaerobic decomposition, which tends to be higher than microbial uptake when soils have C:N ratios below microbial demand (i.e., C:N ratios ≤25; Reddy & DeLaune, 2008), like in our soil samples. The low surface water concentrations of NH_4^+ also suggest that it was produced during decomposition rather than transported in from surface waters. The higher rates of potential microbial decomposition in the ponds (Figure 6) suggests the formation rates of NH_4^+ may be higher in ponds. Furthermore, the absence of plant uptake of NH_4^+ and PO_4^{3-} in the unvegetated ponds likely contributed to higher nutrient concentrations following wetland loss. Ammonium is the preferred inorganic nitrogen source for marsh plants like *Spartina* (Bowen et al., 2020; Mendelssohn, 1979) and porewater PO_4^{3-} is used as a source of phosphorus (Patrick & DeLaune, 1977). Therefore, the progressive increase in porewater NH_4^+ and PO_4^{3-} in ponds is likely driven by ongoing release through iron reduction (PO_4^{3-}) and organic matter decomposition (NH_4^+) in the absence of corresponding plant uptake (*sensu* Krask et al., 2022; Walker et al., 2022).

4.2. Mechanisms Controlling Greenhouse Gas Production in Vegetated Marshes and Open Water Ponds

We observed higher potential rates of soil carbon decomposition after conversion of vegetated marshes to open water ponds, driven by increases in CO_2 fluxes without corresponding changes in CH_4. This result is consistent with the predictions of higher CO_2 fluxes from open water ponds using a model calibrated to soil carbon densities at our field site (Schoolmaster et al., 2022a). Our observed increases in porewater NH_4^+ and PO_4^{3-} (Figure 4) and decreases in soil organic matter concentrations (Figure 2) also suggest ongoing decomposition after vertical drowning and wetland loss. Our PLS regression approach indicated strong relationships between organic matter availability—and to a lesser extent, chemistry—and methane production (Figure 5), whereas CO_2 production was most related to changes in soil redox potential driven by vegetation loss following vertical drowning (Figure 6).

Redox potential is a master variable that is often correlated with rates of greenhouse gas release in wetland soils, as it reflects the relative abundance of terminal electron acceptors (i.e., oxidants) and donors (i.e., reductants) that drive anaerobic decomposition (Reddy & DeLaune, 2008). Decomposition rates typically increase with redox potential as terminal electron acceptors become available, allowing for more energetically favorable anaerobic and aerobic respiratory pathways (i.e., SO_4^{3-}, Fe oxides, Mn oxides, NO_3^-, then oxygen; McLatchey & Reddy, 1998). This relationship is in direct contrast to our results, where we observed greater CO_2 release from soils with lower redox potentials (i.e., in the ponds, Figure 6). In highly reducing soils—like the marsh and pond soils in our study—methanogenesis and fermentation are the assumed dominant respiratory pathways, although sulfate and nitrate reduction still co-occur (Neubauer & Megonigal, 2021; Vile et al., 2003). In these highly reduced soils, decomposition rates can be decoupled from redox potential (Stagg et al., 2017) or decoupled from the availability of terminal electron acceptors if there is an insufficient supply of electron donors (i.e., oxidized carbon substrates; Boye et al., 2017; D'Angelo & Reddy, 1999; Sutton-Grier et al., 2011). The small but significant contributions of NH_4^+, PO_4^{3-} and DOC concentrations identified in the PLS model suggest that higher carbon and nutrient availability after wetland loss may result in higher soil CO_2 fluxes after vertical drowning (*sensu* Bulseco et al., 2019; Jones et al., 2018; Kirwan et al., 2013). Because the majority of the variance in CO_2 production was unexplained by our measured variables, CO_2 dynamics could have also been driven by unmeasured variables like: the supply of electron donors; other terminal electron acceptors (e.g., Fe(III) or organics like phenolics; Keller & Takagi, 2013; Hodgkins et al., 2014); the influence of other primary producers like benthic microalgae or macroalgae (Spivak et al., 2018); or other environmental variables (e.g., bioturbation; Kostka et al., 2002) that are mediated by the loss of vegetation and can influence CO_2 produced during incubations. Nonetheless, our results indicate that decomposition is progressing at a similar or elevated rate after

vertical drowning, which is decreasing soil carbon concentrations (Figure 2a). Although depth-integrated soil carbon stocks measured from the sediment surface to 1 m depth are not decreased following vertical drowning across the timescale of our study, both modeling results (Schoolmaster et al., 2022b) and our data suggest sustained decomposition following wetland loss should lead to future soil carbon losses.

In contrast to other tidal wetlands, surface soils of the vegetated marshes and open water ponds produced CH_4 throughout the incubation, and methanogenesis was not inhibited by sulfate reducing bacteria outcompeting methanogens for organic substrates (Lovley & Klug, 1983; Stefanie et al., 1994). At the time of sampling, salinity was 6.9 ppt (CPRA of Louisiana, 2024) and SO_4^{3-}concentrations were well below the 1–4 mM threshold that inhibits methanogenesis (Bartlett et al., 1987; Poffenbarger et al., 2011), suggesting CH_4 production may occur in these saline marshes in the summer and early fall, or in response to non-seasonal drivers of salinity (e.g., variation in Mississippi River discharges or local rainfall; Hu et al., 2023; Ou et al., 2020). On average, the surface soils in both vegetated marshes and open water ponds produced about 0.10 μmol CH_4 m^{-2} s^{-1} during the incubation, comparable to the 0.15 μmol CH_4 m^{-2} s^{-1} summer CH_4 flux rates measured using chambers in brackish marshes in Louisiana (Holm et al., 2016; Krauss et al., 2016). Like other ecosystems, we would expect a strong seasonality in CH_4 production (*sensu* McNicol et al., 2017, 2020), with lower CH_4 fluxes in the winter due to higher salinities that typically peak between November and February (CPRA of Louisiana, 2024) and lower temperatures that slow microbial decomposition (Knox et al., 2019). But for this summer sampling, CH_4 represented around 30% of carbon respired in the surface soils (>25 cm), but less than 1% of the carbon respired from deeper soils (Supporting Information S1). Both redox potential and porewater SO_4^{3-} and NO_3^- concentrations remained low or decreased with depth, indicating anaerobic respiration would proceed by fermentation and/or methanogenesis regardless of depth.

The question remains as to why we only observed CH_4 production from surface soils. Other studies provide evidence that CH_4 production in organic soils is related to organic matter availability and chemistry, which is in line with our PLS regression model (Figure 5). Although there were marginal increases in the relative abundance of polysaccharides after wetland loss, the most pronounced differences in organic matter chemistry were the consistent decreases in lignin: polysaccharide ratios with depth in both marshes and ponds (Figure 3a, Supporting Information S1), indicating surface soils of the vegetated marshes and open water ponds contain more easily degradable organics. In anoxic organic soils, CH_4 production increases with the availability of easily degradable carbon sources like polysaccharides, root exudates, or organic matter deposited from decomposing phytoplankton (Bridgham et al., 2013; King et al., 2002; Wang et al., 2023; Yagi & Minami, 1990; Yavitt et al., 1997). Lower-than-expected CH_4 production rates relative to CO_2—like we observed at depth—have been attributed to the use of organics (i.e., phenolics) as a terminal electron acceptors, and a buildup of fermentation products (e.g., CO_2, acetate, H_2) without conversion to CH_4 by methanogens (Bridgham et al., 2013; Miller et al., 2015; Ye et al., 2012). Alternatively, patterns in CH_4 release with depth may have been mediated by changes in microbial functional capacity with depth. CH_4 fluxes from wetlands can be directly linked to the abundance of genes or microorganisms associated with methanogenesis (Woodcroft et al., 2018; Yarwood, 2018; Zhou et al., 2022), and can increase with the abundance of microbial groups that decompose easily degradable carbon (and provide low molecular carbon substrates for methanogenesis; Hou et al., 2000). Fluctuating redox, pH, and/or salinity in surface soils of ponds and vegetated marshes could result in a soil microbiome that increases the availability of methanogenic substrates, leading to CH_4 production (Wang et al., 1993; Wilmoth et al., 2021). Regardless of whether the CH_4 production is mediated by microorganisms through their metabolic capacity, and/or (as our results suggest) indirectly through organic matter availability and decomposability, our results suggest the surface soils of these tidal marshes and ponds are a potential source of CH_4.

5. Conclusions

Coastal wetlands store large soil carbon pools but are vulnerable to loss due to disturbance and climate driven environmental changes (Baustian et al., 2021; Chmura et al., 2003; Davidson, 2014; DeLaune & White, 2012). Our study shows that after vegetated marshes vertically drown and convert into unvegetated open water ponds, soil decomposition continues with higher potential rates of CO_2 release through the soil profile but similar rates of CH_4 production from surface soils. The ongoing decomposition following wetland loss results in lower soil organic matter concentrations and the progressive accumulation of end products of microbial decomposition (i.e., NH_4^+, PO_4^{3-}). In line with our hypothesis, we measured greater potential decomposition rates immediately (within 1–3 years) following vegetation death and wetland loss, but the increase in CO_2 production was not

primarily driven by increased organic matter decomposability and nutrient availability. Instead, CO_2 production was driven by rapid decreases in redox potential (~30%) and by unmeasured variables (~70%) associated with the loss of vegetation following vertical drowning. The inverse relationship between CO_2 production and redox potential is atypical (Reddy & DeLaune, 2008), and likely results from the vegetated wetland soils being anoxic and highly reduced prior to flooding, and therefore dominated by the same anaerobic respiratory pathways as pond soils. Wetlands that are transitioning from higher redox potentials (e.g., +100 mV) may not show the same stimulation of decomposition on flooding (*sensu* Chen et al., 2018; LaCroix et al., 2019). But in this area, where the vegetated wetland soils are highly reduced, we expect that ongoing wetland loss will result in continued losses of previously accreted soil organics and could influence the magnitude and direction of carbon fluxes that are important in global carbon budgets.

Conflict of Interest

The authors declare no conflicts of interest relevant to this study.

Data Availability Statement

The data sets generated for this study can be found in Stagg et al. (2024) at https://doi.org/10.5066/P9YJ25DP.

Acknowledgments
Any use of trade, firm, or product names is for descriptive purposes only and does not imply endorsement by the U.S. Government. This work was supported by U.S. Geological Survey LandCarbon Program, the U.S. Geological Survey South Central Climate Adaptation Science Center, and the U.S. Geological Survey Land Change Science Program within the Ecosystems Mission Area. We gratefully acknowledge Laura Scott for assistance with field sampling, Dawnika Blatter for access to the FTIR spectrometer, Allegra Baird for assistance running samples on the FTIR, Jack McFarland for assistance in sectioning cores, and Lauren Holzman for revising Figure 1.

References

Bartlett, K. B., Bartlett, D. S., Harriss, R. C., & Sebacher, D. I. (1987). Methane emissions along a salt marsh salinity gradient. *Biogeochemistry*, *4*(3), 183–202. https://doi.org/10.1007/BF02187365

Bates, D., Mächler, M., Bolker, B., & Walker, S. (2015). Fitting linear mixed-effects models using lme4. *Journal of Statistical Software*, *67*, 1–48. https://doi.org/10.18637/jss.v067.i01

Baustian, M. M., Stagg, C. L., Perry, C. L., Moss, L. C., & Carruthers, T. J. B. (2021). Long-term carbon sinks in marsh soils of coastal Louisiana are at risk to wetland loss. *Journal of Geophysical Research: Biogeosciences*, *126*(3), e2020JG005832. https://doi.org/10.1029/2020JG005832

Blum, M., Rahn, D., Frederick, B., & Polanco, S. (2023). Land loss in the Mississippi River Delta: Role of subsidence, global sea-level rise, and coupled atmospheric and oceanographic processes. *Global and Planetary Change*, *222*, 104048. https://doi.org/10.1016/j.gloplacha.2023.104048

Bourne, J. (2000). Louisiana's vanishing wetlands: Going, going. *Science*, *289*(5486), 1860–1863. https://doi.org/10.1126/science.289.5486.1860

Bowen, J. L., Giblin, A. E., Murphy, A. E., Bulseco, A. N., Deegan, L. A., Johnson, D. S., et al. (2020). Not all nitrogen is created equal: Differential effects of nitrate and ammonium enrichment in coastal wetlands. *BioScience*, *70*(12), 1108–1119. https://doi.org/10.1093/biosci/biaa140

Boye, K., Noël, V., Tfaily, M. M., Bone, S. E., Williams, K. H., Bargar, J. R., & Fendorf, S. (2017). Thermodynamically controlled preservation of organic carbon in floodplains. *Nature Geoscience*, *10*(6), 415–419. Article 6. https://doi.org/10.1038/ngeo2940

Bridgham, S. D., Cadillo-Quiroz, H., Keller, J. K., & Zhuang, Q. (2013). Methane emissions from wetlands: Biogeochemical, microbial, and modeling perspectives from local to global scales. *Global Change Biology*, *19*(5), 1325–1346. https://doi.org/10.1111/gcb.12131

Bulseco, A. N., Giblin, A. E., Tucker, J., Murphy, A. E., Sanderman, J., Hiller-Bittrolff, K., & Bowen, J. L. (2019). Nitrate addition stimulates microbial decomposition of organic matter in salt marsh sediments. *Global Change Biology*, *25*(10), 3224–3241. https://doi.org/10.1111/gcb.14726

Cadigan, J. A., Jafari, N. H., Stagg, C. L., Laurenzano, C., Harris, B. D., Meselhe, A. E., et al. (2022). Characterization of vegetated and ponded wetlands with implications towards coastal wetland marsh collapse. *Catena*, *218*, 106547. https://doi.org/10.1016/j.catena.2022.106547

Calderón, F., Haddix, M., Conant, R., Magrini-Bair, K., & Paul, E. (2013). Diffuse-reflectance fourier-transform mid-infrared spectroscopy as a method of characterizing changes in soil organic matter. *Soil Science Society of America Journal*, *77*(5), 1591–1600. https://doi.org/10.2136/sssaj2013.04.0131

Catallo, W. J. (1999). Hourly and daily variation of sediment redox potential in tidal wetland sediments. In *Biological resources division biological science report USGS/BRD/BSR-1999-0001* (p. 10). U.S. Geological Survey.

Chambers, L. G., Steinmuller, H. E., & Breithaupt, J. L. (2019). Toward a mechanistic understanding of "peat collapse" and its potential contribution to coastal wetland loss. *Ecology*, *100*(7), e02720. https://doi.org/10.1002/ecy.2720

Chen, H., Zou, J., Cui, J., Nie, M., & Fang, C. (2018). Wetland drying increases the temperature sensitivity of soil respiration. *Soil Biology and Biochemistry*, *120*, 24–27. https://doi.org/10.1016/j.soilbio.2018.01.035

Chmura, G. L., Anisfeld, S. C., Cahoon, D. R., & Lynch, J. C. (2003). Global carbon sequestration in tidal, saline wetland soils. *Global Biogeochemical Cycles*, *17*(4), 1111. https://doi.org/10.1029/2002GB001917

Choi, Y., & Wang, Y. (2004). Dynamics of carbon sequestration in a coastal wetland using radiocarbon measurements. *Global Biogeochemical Cycles*, *18*(4), GB4016. https://doi.org/10.1029/2004GB002261

Coastal Protection and Restoration Authority (CPRA) of Louisiana. (2024). Coastwide reference monitoring system-wetlands monitoring data. Retrieved from coastal information management system (CIMS) database [Dataset]. *CPRA*. Retrieved from http://cims.coastal.louisiana.gov

Coleman, K., & Jenkinson, D. S. (1996). *ROTHC-26.3. A model for the turnover of carbon in soil. Model description and windows users guide*. IACR—Rothamsted.

Couvillion, B. R., Beck, H., Schoolmaster, D., & Fischer, M. (2017). Land area change in coastal Louisiana (1932 to 2016). In *Land area change in coastal Louisiana (1932 to 2016) (USGS numbered series 3381; scientific investigations map)* (Vol. 3381). U.S. Geological Survey. https://doi.org/10.3133/sim3381

D'Angelo, E. M., & Reddy, K. R. (1999). Regulators of heterotrophic microbial potentials in wetland soils. *Soil Biology and Biochemistry*, *31*(6), 815–830. https://doi.org/10.1016/S0038-0717(98)00181-3

Davidson, N. C. (2014). How much wetland has the world lost? Long-term and recent trends in global wetland area. *Marine and Freshwater Research*, *65*(10), 934–941. https://doi.org/10.1071/MF14173

de la Cruz, A. A., Hackney, C. T., & Bhardwaj, N. (1989). Temporal and spatial patterns of redox potential (Eh) in three tidal marsh communities. *Wetlands*, *9*(2), 181–190. https://doi.org/10.1007/BF03160743

DeLaune, R. D., Nyman, J. A., & Patrick, W. H., Jr. (1994). Peat collapse, ponding and wetland loss in a rapidly submerging coastal marsh. *Journal of Coastal Research*, *10*(4), 1021–1030.

DeLaune, R. D., & White, J. R. (2012). Will coastal wetlands continue to sequester carbon in response to an increase in global sea level?: A case study of the rapidly subsiding Mississippi River Deltaic plain. *Climatic Change*, *110*(1), 297–314. https://doi.org/10.1007/s10584-011-0089-6

Duarte, C. M., Dennison, W. C., Orth, R. J. W., & Carruthers, T. J. B. (2008). The charisma of coastal ecosystems: Addressing the imbalance. *Estuaries and Coasts*, *31*(2), 233–238. https://doi.org/10.1007/s12237-008-9038-7

Fagherazzi, S., Mariotti, G., Leonardi, N., Canestrelli, A., Nardin, W., & Kearney, W. S. (2020). Salt marsh dynamics in a period of accelerated sea level rise. *Journal of Geophysical Research: Earth Surface*, *125*(8), e2019JF005200. https://doi.org/10.1029/2019JF005200

Faulkner, S. P., PatrickGambrell, W. R. W. H., & Gambrell, R. P. (1989). Field techniques for measuring wetland soil parameters. *Soil Science Society of America Journal*, *53*(3), 883–890. https://doi.org/10.2136/sssaj1989.03615995005300030042x

FitzGerald, D. M., & Hughes, Z. (2019). Marsh processes and their response to climate change and sea-level rise. *Annual Review of Earth and Planetary Sciences*, *47*(1), 481–517. https://doi.org/10.1146/annurev-earth-082517-010255

Guo, T., DeLaune, R. D., & Patrick, W. H. (2000). Iron and manganese transformation in Louisiana salt and brackish marsh sediment. *Communications in Soil Science and Plant Analysis*, *31*(19–20), 2997–3009. https://doi.org/10.1080/00103620009370645

Hamdi, S., Moyano, F., Sall, S., Bernoux, M., & Chevallier, T. (2013). Synthesis analysis of the temperature sensitivity of soil respiration from laboratory studies in relation to incubation methods and soil conditions. *Soil Biology and Biochemistry*, *58*, 115–126. https://doi.org/10.1016/j.soilbio.2012.11.012

Harvey, A. H., & Smith, F. L. (2007). Avoid common pitfalls when using Henry's Law. *NIST*, *103*(9), 33–39.

Haywood, B. J., Hayes, M. P., White, J. R., & Cook, R. L. (2020). Potential fate of wetland soil carbon in a deltaic coastal wetland subjected to high relative sea level rise. *Science of the Total Environment*, *711*, 135185. https://doi.org/10.1016/j.scitotenv.2019.135185

Hodgkins, S. B., Tfaily, M. M., McCalley, C. K., Logan, T. A., Crill, P. M., Saleska, S. R., et al. (2014). Changes in peat chemistry associated with permafrost thaw increase greenhouse gas production. *Proceedings of the National Academy of Sciences of the United States of America*, *111*(16), 5819–5824. https://doi.org/10.1073/pnas.1314641111

Holm, G. O., Perez, B. C., McWhorter, D. E., Krauss, K. W., Johnson, D. J., Raynie, R. C., & Killebrew, C. J. (2016). Ecosystem level methane fluxes from tidal freshwater and brackish marshes of the Mississippi river delta: Implications for coastal wetland carbon projects. *Wetlands*, *36*(3), 401–413. https://doi.org/10.1007/s13157-016-0746-7

Hou, A. X., Chen, G. X., Wang, Z. P., Van Cleemput, O., & Patrick, W. H., Jr. (2000). Methane and nitrous oxide emissions from a rice field in relation to soil redox and microbiological processes. *Soil Science Society of America Journal*, *64*(6), 2180–2186. https://doi.org/10.2136/sssaj2000.6462180x

Howes, B. L., Howarth, R. W., Teal, J. M., & Valiela, I. (1981). Oxidation-reduction potentials in a salt marsh: Spatial patterns and interactions with primary production. *Limnology & Oceanography*, *26*(2), 350–360. https://doi.org/10.4319/lo.1981.26.2.0350

Hu, K., Meselhe, E. A., & Reed, D. J. (2023). Understanding drivers of salinity and temperature dynamics in Barataria Estuary, Louisiana. *Journal of Geophysical Research: Oceans*, *128*(7), e2023JC019635. https://doi.org/10.1029/2023JC019635

Jaynes, M. L., & Carpenter, S. R. (1986). Effects of vascular and nonvascular macrophytes on sediment redox and solute dynamics. *Ecology*, *67*(4), 875–882. https://doi.org/10.2307/1939810

Jones, S. F., Stagg, C. L., Krauss, K. W., & Hester, M. W. (2018). Flooding alters plant-mediated carbon cycling independently of elevated atmospheric CO_2 concentrations. *Journal of Geophysical Research: Biogeosciences*, *123*(6), 1976–1987. https://doi.org/10.1029/2017JG004369

Jones, S. F., Stagg, C. L., Yando, E. S., James, W. R., Buffington, K. J., & Hester, M. W. (2021). Stress gradients interact with disturbance to reveal alternative states in salt marsh: Multivariate resilience at the landscape scale. *Journal of Ecology*, *109*(9), 3211–3223. https://doi.org/10.1111/1365-2745.13552

Keller, J. K., & Takagi, K. K. (2013). Solid-phase organic matter reduction regulates anaerobic decomposition in bog soil. *Ecosphere*, *4*(5), art54-12. https://doi.org/10.1890/ES12-00382.1

King, J. Y., Reeburgh, W. S., Thieler, K. K., Kling, G. W., Loya, W. M., Johnson, L. C., & Nadelhoffer, K. J. (2002). Pulse-labeling studies of carbon cycling in Arctic tundra ecosystems: The contribution of photosynthates to methane emission. *Global Biogeochemical Cycles*, *16*(4), 10-1–10-18. https://doi.org/10.1029/2001GB001456

Kirwan, M. L., Langley, J. A., Guntenspergen, G. R., & Megonigal, J. P. (2013). The impact of sea-level rise on organic matter decay rates in Chesapeake Bay brackish tidal marshes. *Biogeosciences*, *10*(3), 1869–1876. https://doi.org/10.5194/bg-10-1869-2013

Kirwan, M. L., & Megonigal, J. P. (2013). Tidal wetland stability in the face of human impacts and sea-level rise. *Nature*, *504*(7478), 53–60. https://doi.org/10.1038/nature12856

Knox, S. H., Jackson, R. B., Poulter, B., McNicol, G., Fluet-Chouinard, E., Zhang, Z., et al. (2019). FLUXNET-CH4 synthesis activity: Objectives, observations, and future directions. *Bulletin of the American Meteorological Society*, *100*(12), 2607–2632. https://doi.org/10.1175/BAMS-D-18-0268.1

Koretsky, C. M., Haveman, M., Cullear, A., Beuving, L., Shattuck, T., & Wagner, M. (2008). Influence of *Spartina* and *Juncus* on saltwater sediments: I. Pore water geochemistry. *Chemical Geology*, *255*(1–2), 87–99. https://doi.org/10.1016/j.chemgeo.2008.06.013

Kostka, J. E., Roychoudhury, A., & Van Cappellen, P. (2002). Rates and controls of anaerobic microbial respiration across spatial and temporal gradients in saltmarsh sediments. *Biogeochemistry*, *60*(1), 49–76. https://doi.org/10.1023/A:1016525216426

Krask, J. L., Buck, T. L., Dunn, R. P., & Smith, E. M. (2022). Increasing tidal inundation corresponds to rising porewater nutrient concentrations in a southeastern U.S. salt marsh. *PLoS One*, *17*(11), e0278215. https://doi.org/10.1371/journal.pone.0278215

Krauss, K. W., Holm Jr, G. O., Perez, B. C., McWhorter, D. E., Cormier, N., Moss, R. F., et al. (2016). Component greenhouse gas fluxes and radiative balance from two deltaic marshes in Louisiana: Pairing chamber techniques and eddy covariance. *Journal of Geophysical Research: Biogeosciences*, *121*(6), 1503–1521. https://doi.org/10.1002/2015JG003224

LaCroix, R. E., Tfaily, M. M., McCreight, M., Jones, M. E., Spokas, L., & Keiluweit, M. (2019). Shifting mineral and redox controls on carbon cycling in seasonally flooded mineral soils. *Biogeosciences*, *16*(13), 2573–2589. https://doi.org/10.5194/bg-16-2573-2019

Lovley, D. R., & Klug, M. J. (1983). Sulfate reducers can outcompete methanogens at freshwater sulfate concentrations. *Applied and Environmental Microbiology*, *45*(1), 187–192. https://doi.org/10.1128/aem.45.1.187-192.1983

Luk, S., Eagle, M. J., Mariotti, G., Gosselin, K., Sanderman, J., & Spivak, A. C. (2023). Peat decomposition and erosion contribute to pond deepening in a temperate salt marsh. *Journal of Geophysical Research: Biogeosciences*, *128*(2), e2022JG007063. https://doi.org/10.1029/2022JG007063

Luk, S. Y., Todd-Brown, K., Eagle, M., McNichol, A. P., Sanderman, J., Gosselin, K., & Spivak, A. C. (2021). Soil organic carbon development and turnover in natural and disturbed salt marsh environments. *Geophysical Research Letters*, *48*(2), e2020GL090287. https://doi.org/10.1029/2020GL090287

Marschner, P. (2021). Processes in submerged soils—Linking redox potential, soil organic matter turnover and plants to nutrient cycling. *Plant and Soil*, *464*(1), 1–12. https://doi.org/10.1007/s11104-021-05040-6

Materne, M., Bush, T., Houck, M., & Snell, S. (2022). *Plant Guide for smooth cordgrass (*Spartina alterniflora*)*. USDA-National Resources Conservation Serice, Louisiana State Office.

McLatchey, G. P., & Reddy, K. R. (1998). Regulation of organic matter decomposition and nutrient release in a wetland soil. *Journal of Environmental Quality*, *27*(5), 1268–1274. https://doi.org/10.2134/jeq1998.00472425002700050036x

Mcleod, E., Chmura, G. L., Bouillon, S., Salm, R., Björk, M., Duarte, C. M., et al. (2011). A blueprint for blue carbon: Toward an improved understanding of the role of vegetated coastal habitats in sequestering CO_2. *Frontiers in Ecology and the Environment*, *9*(10), 552–560. https://doi.org/10.1890/110004

McNicol, G., Knox, S. H., Guilderson, T. P., Baldocchi, D. D., & Silver, W. L. (2020). Where old meets new: An ecosystem study of methanogenesis in a reflooded agricultural peatland. *Global Change Biology*, *26*(2), 772–785. https://doi.org/10.1111/gcb.14916

McNicol, G., Sturtevant, C. S., Knox, S. H., Dronova, I., Baldocchi, D. D., & Silver, W. L. (2017). Effects of seasonality, transport pathway, and spatial structure on greenhouse gas fluxes in a restored wetland. *Global Change Biology*, *23*(7), 2768–2782. https://doi.org/10.1111/gcb.13580

Mendelssohn, I. A. (1979). Nitrogen metabolism in the height forms of *Spartina alterniflora* in North Carolina. *Ecology*, *60*(3), 574–584. https://doi.org/10.2307/1936078

Miller, K. E., Lai, C.-T., Friedman, E. S., Angenent, L. T., & Lipson, D. A. (2015). Methane suppression by iron and humic acids in soils of the Arctic Coastal Plain. *Soil Biology and Biochemistry*, *83*, 176–183. https://doi.org/10.1016/j.soilbio.2015.01.022

Morris, J. T., Sundareshwar, P. V., Nietch, C. T., Kjerfve, B., & Cahoon, D. R. (2002). Responses of coastal wetlands to rising sea level. *Ecology*, *83*(10), 2869–2877. https://doi.org/10.1890/0012-9658(2002)083[2869:ROCWTR]2.0.CO;2

Mueller, P., Jensen, K., & Megonigal, J. P. (2016). Plants mediate soil organic matter decomposition in response to sea level rise. *Global Change Biology*, *22*(1), 404–414. https://doi.org/10.1111/gcb.13082

National Agricultural Imagery Program (NAIP). (2024). USA NAIP imagery: Color infrared [Dataset]. *NAIP on AWS*. Retrieved from https://registry.opendata.aws/naip

Nelson, D. W., & Sommers, L. E. (1996). Total carbon, organic carbon, and organic matter. In *Methods of soil analysis* (pp. 961–1010). John Wiley & Sons, Ltd. https://doi.org/10.2136/sssabookser5.3.c34

Neubauer, S. C., Franklin, R. B., & Berrier, D. J. (2013). Saltwater intrusion into tidal freshwater marshes alters the biogeochemical processing of organic carbon. *Biogeosciences*, *10*(12), 8171–8183. https://doi.org/10.5194/bg-10-8171-2013

Neubauer, S. C., & Megonigal, J. P. (2021). Biogeochemistry of wetland carbon preservation and flux. In *Wetland carbon and environmental management* (pp. 33–71). American Geophysical Union (AGU). https://doi.org/10.1002/9781119639305.ch3

Nyman, J. A., DeLaune, R. D., Roberts, H. H., & Patrick, W. H. (1993). Relationship between vegetation and soil formation in a rapidly submerging coastal marsh. *Marine Ecology Progress Series*, *96*(3), 269–279. https://doi.org/10.3354/meps096269

Ou, Y., Xue, Z. G., Li, C., Xu, K., White, J. R., Bentley, S. J., & Zang, Z. (2020). A numerical investigation of salinity variations in the Barataria Estuary, Louisiana in connection with the Mississippi River and restoration activities. *Estuarine, Coastal and Shelf Science*, *245*, 107021. https://doi.org/10.1016/j.ecss.2020.107021

Parikh, S. J., Goyne, K. W., Margenot, A. J., Mukome, F. N. D., & Calderón, F. J. (2014). Chapter one—Soil chemical insights provided through vibrational spectroscopy. In D. L. Sparks (Ed.), *Advances in agronomy* (Vol. 126, pp. 1–148). Academic Press. https://doi.org/10.1016/B978-0-12-800132-5.00001-8

Parton, W. J., Ojima, D. S., Cole, C. V., & Schimel, D. S. (1994). A general model for soil organic matter dynamics: Sensitivity to litter chemistry, texture and management. In *Quantitative modeling of soil forming processes* (pp. 147–167). John Wiley & Sons, Ltd. https://doi.org/10.2136/sssaspecpub39.c9

Patrick, W. H., & DeLaune, R. D. (1977). Chemical and biological redox systems affecting nutrient availability in the coastal wetlands. *Geosicence and Man*, *XVIII*, 113–117.

Patton, C. J., & Kryskalla, J. R. (2011). *Colorimetric determination of nitrate plus nitrite in water by enzymatic reduction, automated discrete analyzer methods (5-B8; techniques and methods)* (p. 34). U.S. Geological Survey Office of Water Quality, National Water Quality Laboratory.

Paul, E. A., Morris, S. J., & Böhm, S. (2001). The determination of soil C pool sizes and turnover rates: Biophysical fractionation and tracers. In R. Lal, J. M. Kimble, R. F. Follett, & B. A. Stewart (Eds.), *Assessment methods for soil carbon* (pp. 193–205). Lewis Publ.

Poffenbarger, H. J., Needelman, B. A., & Megonigal, J. P. (2011). Salinity influence on methane emissions from tidal marshes. *Wetlands*, *31*(5), 831–842. https://doi.org/10.1007/s13157-011-0197-0

R Core Team. (2014). R: A language and environment for statistical computing [Computer software]. *R Core Team*. Retrieved from http://www.R-project.org

Reddy, K. R., D'Angelo, E. M., & Harris, W. G. (2000). Biogeochemistry of wetlands. In *Handbook of soil science* (pp. G89–G119). CRC Press.

Reddy, K. R., & DeLaune, R. D. (2008). *Biogeochemistry of wetlands: Science and applications*. CRC Press.

Saintilan, N., Kovalenko, K. E., Guntenspergen, G., Rogers, K., Lynch, J. C., Cahoon, D. R., et al. (2022). Constraints on the adjustment of tidal marshes to accelerating sea level rise. *Science*, *377*(6605), 523–527. https://doi.org/10.1126/science.abo7872

Sander, R. (2015). Compilation of Henry's law constants (version 4.0) for water as solvent. *Atmospheric Chemistry and Physics*, *15*(8), 4399–4981. https://doi.org/10.5194/acp-15-4399-2015

Sapkota, Y., & White, J. R. (2021). Long-term fate of rapidly eroding carbon stock soil profiles in coastal wetlands. *Science of the Total Environment*, *753*, 141913. https://doi.org/10.1016/j.scitotenv.2020.141913

Schädel, C., Luo, Y., David Evans, R., Fei, S., & Schaeffer, S. M. (2013). Separating soil CO_2 efflux into C-pool-specific decay rates via inverse analysis of soil incubation data. *Oecologia*, *171*(3), 721–732. https://doi.org/10.1007/s00442-012-2577-4

Schmidt, M. W. I., Torn, M. S., Abiven, S., Dittmar, T., Guggenberger, G., Janssens, I. A., et al. (2011). Persistence of soil organic matter as an ecosystem property. *Nature*, *478*(7367), 49–56. https://doi.org/10.1038/nature10386

Schoolmaster, D. R., Stagg, C. L., Creamer, C., Laurenzano, C., Ward, E. J., Waldrop, M. P., et al. (2022a). A model of the spatiotemporal dynamics of soil carbon following coastal wetland loss applied to a Louisiana Salt Marsh in the Mississippi River Deltaic Plain. *Journal of Geophysical Research: Biogeosciences*, *127*(6), e2022JG006807. https://doi.org/10.1029/2022JG006807

Schoolmaster, D. R., Stagg, C. L., Creamer, C. A., Laurenzano, C., Ward, E. J., Waldrop, M. P., et al. (2022b). Spatiotemporal dynamics of soil carbon following coastal wetland loss at a Louisiana coastal salt marsh in the Mississippi River Deltaic Plain in 2019 [Dataset]. *U.S. Geological Survey*. https://doi.org/10.5066/P916JH3L

Schoolmaster, D. R., Stagg, C. L., Sharp, L. A., McGinnis, T. E., Wood, B., & Piazza, S. C. (2018). Vegetation cover, tidal amplitude and land area predict short-term marsh vulnerability in coastal Louisiana. *Ecosystems*, *21*(7), 1335–1347. https://doi.org/10.1007/s10021-018-0223-7

Spivak, A. C., Gosselin, K. M., & Sylva, S. P. (2018). Shallow ponds are biogeochemically distinct habitats in salt marsh ecosystems. *Limnology & Oceanography*, *63*(4), 1622–1642. https://doi.org/10.1002/lno.10797

Spivak, A. C., Sanderman, J., Bowen, J. L., Canuel, E. A., & Hopkinson, C. S. (2019). Global-change controls on soil-carbon accumulation and loss in coastal vegetated ecosystems. *Nature Geoscience*, *12*(9), 685–692. Article 9. https://doi.org/10.1038/s41561-019-0435-2

Stagg, C. L., Baustian, M. M., Perry, C. L., Carruthers, T. J. B., & Hall, C. T. (2018). Direct and indirect controls on organic matter decomposition in four coastal wetland communities along a landscape salinity gradient. *Journal of Ecology*, *106*(2), 655–670. https://doi.org/10.1111/1365-2745.12901

Stagg, C. L., Creamer, C. A., Waldrop, M. P., Manies, K. L., Baustian, M. M., Laurenzano, C., et al. (2024). Plant, soil, and microbial characteristics of marsh collapse in Mississippi River Deltaic wetlands. *U.S. Geological Survey Data Release*. https://doi.org/10.5066/P9YJ25DP

Stagg, C. L., & Mendelssohn, I. A. (2010). Restoring ecological function to a submerged salt marsh. *Restoration Ecology*, *18*(s1), 10–17. https://doi.org/10.1111/j.1526-100X.2010.00718.x

Stagg, C. L., Osland, M. J., Moon, J. A., Hall, C. T., Feher, L. C., Jones, W. R., et al. (2020). Quantifying hydrologic controls on local- and landscape-scale indicators of coastal wetland loss. *Annals of Botany*, *125*(2), 365–376. https://doi.org/10.1093/aob/mcz144

Stagg, C. L., Schoolmaster, D. R., Krauss, K. W., Cormier, N., & Conner, W. H. (2017). Causal mechanisms of soil organic matter decomposition: Deconstructing salinity and flooding impacts in coastal wetlands. *Ecology*, *98*(8), 2003–2018. https://doi.org/10.1002/ecy.1890

Stefanie, J. W. H. O. E., Visser, A., Pol, L. W. H., & Stams, A. J. M. (1994). Sulfate reduction in methanogenic bioreactors. *FEMS Microbiology Reviews*, *15*(2–3), 119–136. https://doi.org/10.1111/j.1574-6976.1994.tb00130.x

Sutton-Grier, A. E., Keller, J. K., Koch, R., Gilmour, C., & Megonigal, J. P. (2011). Electron donors and acceptors influence anaerobic soil organic matter mineralization in tidal marshes. *Soil Biology and Biochemistry*, *43*(7), 1576–1583. https://doi.org/10.1016/j.soilbio.2011.04.008

Törnqvist, T. E., Jankowski, K. L., Li, Y.-X., & González, J. L. (2020). Tipping points of Mississippi Delta marshes due to accelerated sea-level rise. *Science Advances*, *6*(21), eaaz5512. https://doi.org/10.1126/sciadv.aaz5512

U.S. EPA. (1993a). *Method 350.1: Nitrogen, ammonia (colorimetric, automated phenate), revision 2.0* (p. 15). Environmental Monitoring Systems Laboratory, Office of Research and Development, U.S. Environmental Protection Agency.

U.S. EPA. (1993b). *Method 365.1, revision 2.0: Determination of phosphorus by semi-automated colorimetry* (p. 18). Environmental Monitoring Systems Laboratory, Office of Research and Development, U.S. Environmental Protection Agency. Retrieved from https://www.epa.gov/sites/default/files/2015-08/documents/method_365-1_1993.pdf

U.S. EPA. (2007). *Method 9056A: Determination of inorganic anions by ion chromatography (hazardous waste test methods SW-846)* (p. 19). U. S. Environmental Protection Agency.

Vile, M. A., Bridgham, S. D., & Wieder, R. K. (2003). Response of anaerobic carbon mineralization rates to sulfate amendments in a boreal peatland. *Ecological Applications*, *13*(3), 720–734. https://doi.org/10.1890/1051-0761(2003)013[0720:ROACMR]2.0.CO;2

Waldrop, M. P., McFarland, W., Manies, K. L., Leewis, M. C., Blazewicz, S. J., Jones, M. C., et al. (2021). Carbon fluxes and microbial activities from boreal peatlands experiencing permafrost thaw. *Journal of Geophysical Research: Biogeosciences*, *126*(3), e2020JG005869. https://doi.org/10.1029/2020JG005869

Walker, J. B., Rinehart, S., Greenberg-Pines, G., White, W. K., DeSantiago, R., Lipson, D. A., & Long, J. D. (2022). Aboveground competition influences density-dependent effects of cordgrass on sediment biogeochemistry. *Ecology and Evolution*, *12*(3), e8722. https://doi.org/10.1002/ece3.8722

Wang, T., Zhumabieke, M., Zhang, N., Liu, C., Zhong, J., Liao, Q., & Zhang, L. (2023). Variable promotion of algae and macrophyte organic matter on methanogenesis in anaerobic lake sediment. *Environmental Research*, *237*(1), 116922. https://doi.org/10.1016/j.envres.2023.116922

Wang, Z. P., DeLaune, R. D., Masscheleyn, P. H., & Patrick, W. H. (1993). Soil redox and pH effects on methane production in a flooded rice soil. *Soil Science Society of America Journal*, *57*(2), 382–385. https://doi.org/10.2136/sssaj1993.03615995005700020016x

Wilmoth, J. L., Schaefer, J. K., Schlesinger, D. R., Roth, S. W., Hatcher, P. G., Shoemaker, J. K., & Zhang, X. (2021). The role of oxygen in stimulating methane production in wetlands. *Global Change Biology*, *27*(22), 5831–5847. https://doi.org/10.1111/gcb.15831

Wolf, A. A., Drake, B. G., Erickson, J. E., & Megonigal, J. P. (2007). An oxygen-mediated positive feedback between elevated carbon dioxide and soil organic matter decomposition in a simulated anaerobic wetland. *Global Change Biology*, *13*(9), 2036–2044. https://doi.org/10.1111/j.1365-2486.2007.01407.x

Wood, S. N. (2017). *Generalized additive models: An introduction with R* (2nd ed.). Chapman and Hall/CRC. https://doi.org/10.1201/9781315370279

Woodcroft, B. J., Singleton, C. M., Boyd, J. A., Evans, P. N., Emerson, J. B., Zayed, A. A. F., et al. (2018). Genome-centric view of carbon processing in thawing permafrost. *Nature*, *560*(7716), 49–54. Article 7716. https://doi.org/10.1038/s41586-018-0338-1

Yagi, K., & Minami, K. (1990). Effect of organic matter application on methane emission from some Japanese paddy fields. *Soil Science & Plant Nutrition*, *36*(4), 599–610. https://doi.org/10.1080/00380768.1990.10416797

Yarwood, S. A. (2018). The role of wetland microorganisms in plant-litter decomposition and soil organic matter formation: A critical review. *FEMS Microbiology Ecology*, *94*(11), fiy175. https://doi.org/10.1093/femsec/fiy175

Yavitt, J. B., Williams, C. J., & Wieder, R. K. (1997). Production of methane and carbon dioxide in peatland ecosystems across North America: Effects of temperature, aeration, and organic chemistry of peat. *Geomicrobiology Journal*, *14*(4), 299–316. https://doi.org/10.1080/01490459709378054

Ye, R., Jin, Q., Bohannan, B., Keller, J. K., McAllister, S. A., & Bridgham, S. D. (2012). pH controls over anaerobic carbon mineralization, the efficiency of methane production, and methanogenic pathways in peatlands across an ombrotrophic–minerotrophic gradient. *Soil Biology and Biochemistry*, *54*, 36–47. https://doi.org/10.1016/j.soilbio.2012.05.015

Zhou, J., Theroux, S. M., Bueno de Mesquita, C. P., Hartman, W. H., Tian, Y., & Tringe, S. G. (2022). Microbial drivers of methane emissions from unrestored industrial salt ponds. *The ISME Journal*, *16*(1), 284–295. Article 1. https://doi.org/10.1038/s41396-021-01067-w